21p.

N64-17226*
CODE-1
CR-53196

Technical Report No. 32-534

Determination of Tracking Station Locations by Doppler and Range Measurements to an Earth Satellite

D. L. Cain

T. W. Hamilton

OTS PRICE

XEROX $ 2.60 ph

MICROFILM $ 0.83 mf.

JET PROPULSION LABORATORY
CALIFORNIA INSTITUTE OF TECHNOLOGY
PASADENA, CALIFORNIA

February 1, 1964

(NASA Contract NAS7-100)

(NASA CR-53196; JPL-TR-32-534) OTS: $2.60ph, $0.83mf

[2]

☒ OTS

Technical Report No. 32-534

Determination of Tracking Station Locations by Doppler and Range Measurements to an Earth Satellite

D. L. Cain and

T. W. Hamilton 1 Feb. 1964 21p refs

T. W. Hamilton

T. W. Hamilton, Chief

System Analysis Section

JET PROPULSION LABORATORY

CALIFORNIA INSTITUTE OF TECHNOLOGY

PASADENA, CALIFORNIA

February 1, 1964

1304823

Copyright © 1964
Jet Propulsion Laboratory
California Institute of Technology

Prepared Under Contract No. NAS 7-100
National Aeronautics & Space Administration

CONTENTS

I. Introduction 1

II. Accuracy of Locating Station by Data from a Single Pass . . . 2
- A. Procedure for Cases Examined 2
- B. Numerical Results 2
- C. Significance of Results 3

III. Accuracy of Locating Station by Combined Data from Two Passes 4
- A. Some Numerical Results 4
- B. Significance of Results 4

IV. Reasons for Improvement in Knowledge of Station Coordinates When Passes Are Combined 5
- A. Transformation of Spherical-Coordinate Errors to the Local Cartesian System 5
- B. Numerical Example 5
  - 1. Eigenvalues and Eigenvectors of Transformed Covariances . . 5
  - 2. Relation of Eigenvectors to Pass Geometry 6

V. Critical Accuracy Variation for Single Passes 12
- A. Summary of Single-Pass Results 12
- B. Variations of Middle and Largest Semi-axes with Type of Pass, Latitude, and Altitude 12
  - 1. Variation of Middle Semi-axis with Type of Pass 12
  - 2. Variation of Largest Semi-axis with Latitude and Type of Pass 12
  - 3. Variation of Middle Semi-axis with Latitude 12
  - 4. Variation of Middle Semi-axis with Altitude 12
- C. Comparison of Range and Range-Rate Measurements 12

VI. Conclusions 14
- A. Primary Results 14
- B. Restrictive Assumptions 14
- C. The Total Problem 14

Nomenclature 15

References 15

TABLES

1. Maximum elevation angles for equatorial station 2
2. Sampling rates and assumed data sigmas for equatorial station . . 2
3. Station-coordinate uncertainty, range rate only, satellite east . . . 3
4. Station-coordinate uncertainty, range rate only, satellite west . . . 3
5. Station-coordinate uncertainty, range only, satellite east 3
6. Station-coordinate uncertainty, range only, satellite west 3
7. Station-locating accuracy for selected two-pass situations 4
8. Values of semi-axes and eigenvectors defining their directions . . . 6
9. Properties of 1-σ ellipsoid of combined-pass estimate 6
10. Semi-axes of error ellipsoids for single passes 8

FIGURES

1. Dispersion ellipsoids of station-location error for single passes eastward and westward of station (range rate, equatorial station, satellite altitude = 1860 km) 7
2. Geometry for assumptions of nonoverhead pass and nonrotating Earth 9
3. Satellite–station spherical coordinates 9
4. Relation of measurements determining R and ψ_0 11
5. Variation of middle semi-axis with altitude for overhead pass at equatorial station 12
6. Ranging accuracy required to obtain middle semi-axis equal to that obtainable with range rate of 0.03 m/sec (1-min sampling rate) . . . 13
7. Data standard deviations required to obtain middle semi-axis of 5 m (accuracies normalized to 1-min sampling rate) 13

ABSTRACT

17226 A

The accumulation of accurate tracking data on an Earth satellite which is relatively free from unknown or unpredictable accelerations offers the opportunity to obtain estimates of tracking-station locations, data systematic errors, and the Earth's potential field, together with a precise ephemeris of the satellite. This Report is an examination of a simplified version of the case stated, with attention to the determination of station coordinates.

The accuracy to which the station coordinates may be obtained from the tracking of single and multiple passes by means of range or doppler (range-rate) measurements alone is examined under the assumption that the satellite's orbit is perfectly known. The results indicate that dramatic improvement is attained when data from two different passes are statistically combined. A method is introduced whereby this improvement may be easily understood. The middle semi-axis of the three-dimensional error ellipsoid associated with a single pass is introduced as the most valuable measure of accuracy. The variation of accuracy with satellite altitude, station latitude, data type, and the geometry of the pass is extensively examined.

It is found that the ranging accuracy equivalent to a 0.03-m/sec range-rate accuracy varies from 1.8 m at a satellite altitude of 100 nm to 15.5 m at 1000 nm, and that such data accuracies should permit determination of all three station coordinates to about 5 m when the data from two or more passes are utilized. Author

I. INTRODUCTION

The accuracies obtained in modern systems for tracking space probes and ballistic missiles have become so great that the "systematic errors" have become the dominant type. In order to realize the benefits of this accuracy potential, the systematic errors must be understood and reduced. The only practical procedure is experimental examination of these errors. Recent studies have illustrated the feasibility of calibrating precise ground tracking systems through the tracking of Earth satellites (Ref. 1). It is expected that such studies of systematic errors will permit their elimination or proper inclusion in the statistical estimation of the trajectory.

Although the major purpose of such calibration satellites is to provide a means of examining the systematic errors of the tracking system, it is natural that information of fundamental and practical significance will be obtained: for example, the description of the Earth's gravitational field and the accurate real-time evaluation of integrated atmospheric effects on the radio tracking signals when the satellite is near the horizon. For the tracking of lunar and interplanetary probes, the primary systematic error is that in the station's coordinates. This Report is restricted to an examination of the error statistics associated with the use of a calibration satellite for the purpose of evaluating tracking-station coordinates. In order to illustrate an important aspect of the problem, we have made two important simplifying assumptions: (1) that the satellite's coordinates with respect to the Earth's spin axis and to Greenwich are perfectly known (from analysis of all tracking information), and (2) that all station clocks are perfectly synchronized with Greenwich Mean Time.

In Ref. 1, a single pass was analyzed, and the mean coordinates of the station were treated as perfectly known, a procedure which is entirely appropriate for the case analyzed. In the present case, the orbit is treated as perfectly known, and the station coordinates are found with respect to the orbit (hence, to the basic reference system) for single and multiple passes. The results for single passes, using range data only and doppler data only, are presented in Section II of this Report.

Section III presents the most interesting and, perhaps, surprising results obtained by combining data from separate passes. The reasons for the significant improvement obtainable through the use of data from two or more passes are given in Section IV, together with a more useful way of characterizing single-pass results which allows easy visualization of the favorable geometry associated with combining results of separate passes.

In Section V, we examine the variation in the accuracy of determining the critical middle semi-axis of the concentration ellipsoid of station coordinates for a single pass. The results indicate that the variation of accuracy with satellite maximum elevation and station latitude is relatively small. It is shown that the random error in ranging which produces an accuracy equivalent to 0.03-m/sec doppler is a strong function of satellite altitude, varying from 15.3 m at an altitude of 1860 km (1000 nm) to 1.8 m at 186 km. Data accuracies required to obtain 5-m accuracy in station locating are shown.

In Section VI, the effect of the restrictive assumptions is discussed, and some procedures are suggested for future examinations of this problem.

II. ACCURACY OF LOCATING STATION BY DATA FROM A SINGLE PASS

In the following discussion, we present results summarizing the accuracy to which a station's spherical coordinates may be determined by tracking a single pass of a satellite of perfectly known orbit. The standard deviations in radius, latitude, and longitude are used as measures of the error.

A. Procedure for Cases Examined

The observation vector $\mathbf{y}$ was assumed to depend only on the coordinates $\boldsymbol{\phi}$ of the tracking station. The noise in the observations was assumed to be gaussian and independent from point to point. The minimum-variance linear unbiased estimator of the tracking-station coordinates is, then,

$$\delta\boldsymbol{\phi}^* = (A^TWA)^{-1}A^TW\delta\mathbf{y} \tag{1}$$

where δ represents the deviation from the reference station coordinates or the observable quantities. Here, $\delta\mathbf{y} = A\delta\boldsymbol{\phi}$ and, for small deviations, defines A; W is the inverse of the data-noise covariance matrix; and the superior T denotes the transpose. The statistics of the error in station coordinates are described by

$$\text{covar } \boldsymbol{\phi}^* = (A^TWA)^{-1} \triangleq (J)^{-1} \tag{2}$$

The basic normal matrices J for one orbital pass were computed for each station, data type, satellite altitude, and direction of the pass.

All satellite orbits were circular and inclined at 32 deg. Three orbital altitudes (186 km, 930 km, 1860 km) and five station latitudes, all north, were simulated. Station latitudes were chosen from 0 to 30 deg in 7.5-deg increments. Different station–satellite geometries were investigated by a simple procedure. First, stations were placed in longitude so as to be directly below the satellite's path, thus simulating an overhead pass. For nonoverhead-pass geometry, only the *epoch* of the satellite's initial condition was changed, causing the station to be east (epoch increase) or west (epoch decrease) of the satellite's pass because of the Earth's rotation. The magnitude of epoch change was increased as the satellite's altitude was increased, so as to give a similar geometry for each case. The overhead case is designated by 0, the epoch increase by +, and the epoch decrease (by an equal amount) by −. The resulting maximum elevation angles are given in Table 1 for the equatorial station.

Both range and range-rate observations were simulated, the sampling rates being varied with height. The sampling rates and data sigmas vs altitude are shown in Table 2. The apparent variation of accuracy with altitude is due only to the use of a lower sampling rate at higher altitudes to conserve computer time. If the 2-sec sample spacing had been employed at all altitudes, the data-noise standard deviations would have been identical for all three altitudes: $30\sqrt{30}$ m in range, and $0.03\sqrt{30}$ m/sec in range rate. Use of the factor $\sqrt{30}$ is explained by the fact that, in usual practice, accuracies are stated at a 1-min sample spacing, which is more appropriate for space probes. Thus, the accuracy assumptions are equivalent to 30 m and 0.03 m/sec at one sample per minute.

Table 1. Maximum elevation angles for equatorial station

Altitude, km	Maximum elevation angle, deg	
	Epoch change +	Epoch change −
186	26.9	27.0
930	21.8	21.2
1860	35.1	33.2

Note: Periods are 88, 104, and 124 min, respectively.

Table 2. Sampling rates and assumed data sigmas for equatorial station

Altitude, km	Sample spacing, sec	Range standard deviation, m	Range rate standard deviation, m/sec
186	2	$30\sqrt{30}$	$0.03\sqrt{30}$
930	5	$30\sqrt{12}$	$0.03\sqrt{12}$
1860	10	$30\sqrt{6}$	$0.03\sqrt{6}$

A pass consists of data taken from horizon to horizon. In order to discount data taken where the refraction effects are large, the assumed data variance was increased by 10% of the standard refraction correction at each point.

B. Numerical Results

Tables 3 to 6 summarize the standard deviations in radius, latitude, and longitude for the following cases: range rate, satellite east; range rate, satellite west; range,

Table 3. Station-coordinate uncertainty, range rate only, satellite east

Altitude, km	Station latitude, deg north	Standard deviation of station coordinates		
		Radius, m	Latitude, 10^{-3} deg	Longitude, 10^{-3} deg
186	0	68.0	0.31	0.21
	30	50.8	0.90	0.17
930	0	172.0	0.96	0.58
	30	75.9	2.95	0.17
1860	0	155.0	1.32	0.77
	30	470.0	31.8	3.06

Table 4. Station-coordinate uncertainty, range rate only, satellite west

Altitude, km	Station latitude, deg north	Standard deviation of station coordinates		
		Radius, m	Latitude, 10^{-3} deg	Longitude, 10^{-3} deg
186	0	68.2	0.31	0.21
	30	39.4	0.55	0.17
930	0	164.0	0.94	0.57
	30	61.4	0.64	0.36
1860	0	144.0	1.28	0.76
	30	96.6	1.15	0.70

Table 5. Station-coordinate uncertainty, range only, satellite east

Altitude, km	Station latitude, deg north	Standard deviation of station coordinates		
		Radius, m	Latitude, 10^{-3} deg	Longitude, 10^{-3} deg
186	0	431.0	1.53	1.03
	30	419.0	6.74	1.29
930	0	184.0	0.48	0.32
	30	146.0	4.77	0.29
1860	0	91.6	0.41	0.25
	30	2312.0	155.0	14.9

Table 6. Station-coordinate uncertainty, range only, satellite west

Altitude, km	Station latitude, deg north	Standard deviation of station coordinates		
		Radius, m	Latitude, 10^{-3} deg	Longitude, 10^{-3} deg
186	0	434.0	1.53	1.04
	30	316.0	3.85	1.22
930	0	178.0	0.49	0.32
	30	108.0	0.70	0.41
1860	0	88.0	0.43	0.26
	30	60.3	0.58	0.36

satellite east; and range, satellite west. To conserve space, the results are tabulated for each altitude by only the 0- and 30-deg latitude stations.

C. *Significance of Results*

The standard deviations describing our present knowledge of absolute station locations, excluding satellite and space-probe tracking, are about 60 m in radius and 1×10^{-3} deg in latitude and longitude, with a factor of 2 either way encompassing both the pessimistic and the optimistic viewpoints. A reasonable goal is 5 m in radius and 0.05×10^{-3} deg in latitude and longitude. Some of the results are encouraging; in Table 1, it is suggested that the radius goal can be met for low-altitude satellites and, in Table 2, it is shown that latitude and longitude are obtainable to 0.3×10^{-3} deg and 0.2×10^{-3} deg, respectively. The overall picture, however, appears to be rather discouraging in the case of precise station surveying. To make matters even worse, the results have a very uneven quality and suggest that high-altitude satellites are of little value.

In Section IV, it is demonstrated that moderately good accuracies may be obtained by combining two geometrically dissimilar passes. The basic weakness in the method of describing single-pass results presented in this Section is its failure to suggest this potentiality. The complete results of this study are presented in Section V, using coordinates more suitable than those employed above.

III. ACCURACY OF LOCATING STATION BY COMBINED DATA FROM TWO PASSES

If the vector of observations **y** (see Section II) is augmented to include data from two geometrically dissimilar passes, the covariance of the resulting estimate of station coordinates is significantly altered. Using the nomenclature of Section II, let the normal matrices for passes 1 and 2 over the same station be J_1, J_2, respectively. It is well-known that the error in the ϕ_{12}^* is expressed by

$$\text{covar}\, \phi_{12}^* = (J_1 + J_2)^{-1} \tag{3}$$

Some interesting results of a Monte Carlo simulation of station locating by ranging to a perfectly known satellite were reported by Reich and Schucker (Ref. 2). In the following paragraphs the "dramatic improvement" observed by these authors is described at more length and in a different way. A simple method for understanding and anticipating such results is presented in Section IV.

A. Some Numerical Results

Here, we present enough numerical results to illustrate the significant improvement obtainable by combining two dissimilar passes at a given station. It is not the purpose of this Section to demonstrate how the results vary with data type and satellite orbit parameters (for discussion of that topic, see Section V).

Typical results obtained by combining two passes are listed in Table 7. Here, the standard deviations in radius, latitude, and longitude have again been used as the measure of accuracy. It is interesting to compare the two-pass results with the single-pass results shown in Section II. For the equatorial-station range-rate case at the 1860-km altitude, the single-pass standard deviations in radius, latitude, and longitude are: 144 m, 1.3×10^{-3} deg, and 0.8×10^{-3} deg for probe east; and 155 m, 1.3×10^{-3} deg, and 0.8×10^{-3} deg for probe west. The two passes combined give 6.5 m, 0.058×10^{-3} deg, and 0.041×10^{-3} deg, respectively: an apparent improvement by a factor of 20. Similar situations have been observed in numerous other cases.

B. Significance of Results

It appears that the accuracy goals suggested in Section II can be met without significant increase in the data accuracies assumed, provided that data from two or more passes are combined. Before pursuing that point further, we shall endeavor to provide a simple explanation of the improvement, which is not "dramatic" if the single-pass results are viewed correctly. In order to do this, we transform the errors to a local Cartesian-coordinate system and examine the properties of the three-dimensional concentration ellipsoids which may be used to visualize the uncertainties (Ref. 3).

Table 7. Station-locating accuracy for selected two-pass situations

Satellite altitude, km	Data type	Station latitude, deg north	Types of passes combined	Standard deviation of station coordinates		
				Radius, m	Latitude, 10^{-3} deg	Longitude, 10^{-3} deg
186	Range rate	0	+, −	3.77	0.018	0.014
		30	+, −	1.59	0.025	0.010
	Range	0	+, −	36.7	0.148	0.137
		30	+, −	22.9	0.315	0.144
930	Range rate	0	+, −	8.29	0.048	0.035
		30	+, −	3.24	0.047	0.021
	Range	0	+, −	23.8	0.082	0.096
		30	+, −	22.2	0.168	0.098
1860	Range rate	0	+, −	6.51	0.059	0.041
		30	+, −	12.4	0.234	0.149
	Range	0	+, −	11.6	0.063	0.065
		30	+, −	12.8	0.136	0.078

IV. REASONS FOR IMPROVEMENT IN KNOWLEDGE OF STATION COORDINATES WHEN PASSES ARE COMBINED

The results presented in Section III clearly illustrate the fact that all three coordinates of a station's location may be determined to high accuracy if data from two dissimilar passes are combined. This would appear somewhat surprising if our understanding of the single-pass results were limited to that provided in Section II, where the standard deviations of radius, latitude, and longitude were used as measures of the error. In this Section, we consider covar $\boldsymbol{\varphi}$ in a local Cartesian-coordinate system centered at the nominal station location. In order to distinguish between the two systems, the station-coordinate vector in the new system is denoted by $\mathbf{x}$.

We then examine the ellipsoid of concentration associated with covar $\mathbf{x} \triangleq \Gamma_x$ in order to obtain an understanding of the favorable combination of two passes. The quadratic form $\delta\mathbf{x}^T\Gamma_x^{-1}\delta\mathbf{x} = 1$ is designated as the 1-σ error ellipsoid. This technique is well described in textbooks on mathematical statistics. In order to understand how two passes with single-pass covariance matrices Γ_{x_1}, Γ_{x_2} combine, it is only necessary to realize that the 1-σ ellipsoid, $\delta\mathbf{x}^T\,\Gamma_{x_{12}}^{-1}\,\delta\mathbf{x} = 1$ associated with the combined estimate must be interior (or tangent) to the 1-σ ellipsoids associated with Γ_{x_1} and Γ_{x_2}.

In the following calculation, it will be established that the single-pass ellipsoids are always cigar-shaped, so that the two shorter axes are small in relation to the length. The orientation of the long axis indicates the direction for which no good information is available. We have found that, quite naturally, the direction in which the ellipsoid points can be correlated with the geometry of the pass. Where differences in geometry are present on two passes, the largest semi-axes of the two ellipsoids are nearly orthogonal, and the region interior to both "cigars" is relatively small. The missing information from the first pass is supplied by the second pass.

It thus becomes evident that, for the multiple-pass situation, the figure which best describes the quality of the determination is not the long axis but, rather, the middle-sized axis. The size of the middle semi-axis (MSA) describes the quality of the most useful information, whereas the largest semi-axis (LSA) supplies the more sterile information: i.e., just how poorly the third coordinate is known. For the multiple-pass case, the LSA for a single pass is not important, since substantially all the information for determining that coordinate will come from a subsequent pass.

In order to illustrate the method, we examine a typical case in some detail. Once the approach is clear, many generalizations may be made. A primary purpose of this development is to illustrate how multiple-pass geometric advantage can be understood and expressed. Although the point is not stressed, it is also true that other types of observations taken on the same single pass may result in 1-σ ellipsoids in which the largest semi-axes are nearly orthogonal to the LSA of the range or range-rate ellipsoid. It is obvious that precise angular observations fulfill this condition.

A. Transformation of Spherical-Coordinate Errors to the Local Cartesian System

In this computation, let $(r, \phi, \lambda)^T$ denote the station coordinates $\boldsymbol{\varphi}$ in the radius-latitude-longitude system, and $(x_1, x_2, x_3)^T = \mathbf{x}$ denote the east, north (both in the local horizontal plane), and local vertical directions. Small perturbations in these coordinates are related by

$$\delta\mathbf{x} = \begin{pmatrix} \delta x_1 \\ \delta x_2 \\ \delta x_3 \end{pmatrix} = \begin{bmatrix} 0 & 0 & \dfrac{\pi\, r \cos\phi}{180} \\ 0 & \dfrac{\pi r}{180} & 0 \\ 1 & 0 & 0 \end{bmatrix} \begin{pmatrix} \delta r \\ \delta\phi \\ \delta\lambda \end{pmatrix} = B\delta\boldsymbol{\varphi} \tag{4}$$

If covar $\boldsymbol{\varphi} = \Gamma_\phi$ is known, covar $\mathbf{x}$ may be easily obtained by the relationship

$$\text{covar}\,\mathbf{x} = \Gamma_x = B\,\Gamma_\phi\,B^T \tag{5}$$

The purpose of this transformation is to put all the coordinates in the same dimensions to facilitate interpretation of the 1-σ ellipsoids.

B. Numerical Example

1. Eigenvalues and Eigenvectors of Transformed Covariances

The numerical example we present here is that of an equatorial station taking range-rate data for the following cases: satellite east (−), and satellite west (+). The covariance matrices Γ_{ϕ_+}, Γ_{ϕ_-}, transformed to the $\mathbf{x}$ system, are shown below:

$$\text{covar}\,\mathbf{x}_+ = \begin{pmatrix} 7.2012700\,\text{E}-3 & 1.2060016\,\text{E}-2 & 1.2211694\,\text{E}-2 \\ & 2.0267948\,\text{E}-2 & 2.0503977\,\text{E}-2 \\ \text{(Symmetric)} & & 2.0828316\,\text{E}-2 \end{pmatrix} \text{km}^2$$

$$\text{covar}\,\mathbf{x}_- = \begin{pmatrix} 7.4103073\,\text{E}-3 & 1.2597053\,\text{E}-3 & -1.3336902\,\text{E}-3 \\ & 2.1488987\,\text{E}-2 & -2.2730572\,\text{E}-2 \\ \text{(Symmetric)} & & 2.4138522\,\text{E}-2 \end{pmatrix} \text{km}^2 \tag{6}$$

The square roots of the largest, middle, and smallest eigenvalues correspond to the LSA, MSA, and SSA (smallest semi-axis) of the 1-σ error ellipsoids. The values of the various semi-axes and the unit vectors (eigenvectors) defining their directions are listed in Table 8. The 1-σ ellipsoid of the combined estimate has the properties listed in Table 9.

Table 8. Values of semi-axes and eigenvectors defining their directions

Semi-axis	Value, m	Direction cosine of eigenvector		
		x_1	x_2	x_3
LSA (+)	220	0.386	0.648	0.657
LSA (−)	230	0.374	0.637	−0.675
MSA (+)	6.7	−0.336	−0.564	0.754
MSA (−)	7.0	−0.340	−0.583	−0.738
SSA (+)	4.3	0.859	−0.511	0.000
SSA (−)	4.4	0.863	−0.505	0.002

Table 9. Properties of 1-σ ellipsoid of combined-pass estimate

Semi-axis	Value, m	Direction cosine of eigenvector		
		x_1	x_2	x_3
LSA	7.3	0.505	0.856	0.110
MSA	6.5	−0.056	−0.095	0.994
SSA	3.1	0.861	−0.508	0.000

Inspection of the single-pass LSA and MSA reveals that the horizontal-plane components of the LSA and MSA are substantially the same, but that the vertical components are opposite. The SSA values are virtually identical in both cases. The error ellipsoids are shown in Fig. 1.

2. Relation of Eigenvectors to Pass Geometry

Insight to the problem can be gained by first considering an overhead pass with a nonrotating Earth. Clearly, the station could be horizontally displaced by a small distance in a direction normal to the plane of motion (i.e., the $\boldsymbol{\rho} \times \mathbf{V}$ direction, $\boldsymbol{\rho}$ being the station-to-probe vector, and $\mathbf{V}$ being the satellite velocity), and no change would occur in the data. This implies an infinite semi-axis in this direction. However, a small horizontal displacement of the station in the probe-motion direction when the probe is overhead would result in a maximum change, so that this direction is well determined.

The addition of the Earth's rotation removes the perfect coplanarity of the $\boldsymbol{\rho}$ and $\mathbf{V}$ vectors; therefore, rather than infinite uncertainty in the $\boldsymbol{\rho} \times \mathbf{V}$ direction, a large finite uncertainty is expected and is verified in Table 10.

For a nonoverhead pass and a nonrotating Earth, the geometrical considerations are more complicated, but some of the determining considerations are found from more careful analysis of the principles stated above. The sensitivity of a given doppler measurement D to the station's position may be described by the vector ∇D (gradient of D). The doppler measurement is equivalent to range-rate, or

$$D = \frac{\mathbf{V} \cdot \boldsymbol{\rho}}{|\boldsymbol{\rho}|} \tag{7}$$

where $\mathbf{V}$ = satellite velocity vector and $\boldsymbol{\rho}$ = station-to-probe vector. For the geometry, see Fig. 2, where $\mathbf{r}$ is the Earth-center-to-satellite vector.

Then, differentiating and assuming $\mathbf{r}$ fixed,

$$\nabla D = \frac{(\mathbf{V} \cdot \boldsymbol{\rho})}{|\boldsymbol{\rho}|^3}\,\boldsymbol{\rho} - \frac{1}{|\boldsymbol{\rho}|}\,\mathbf{V} \tag{8}$$

This gradient vector describes the direction along which a small fixed-magnitude displacement of the station would yield a maximum doppler change (most sensitive

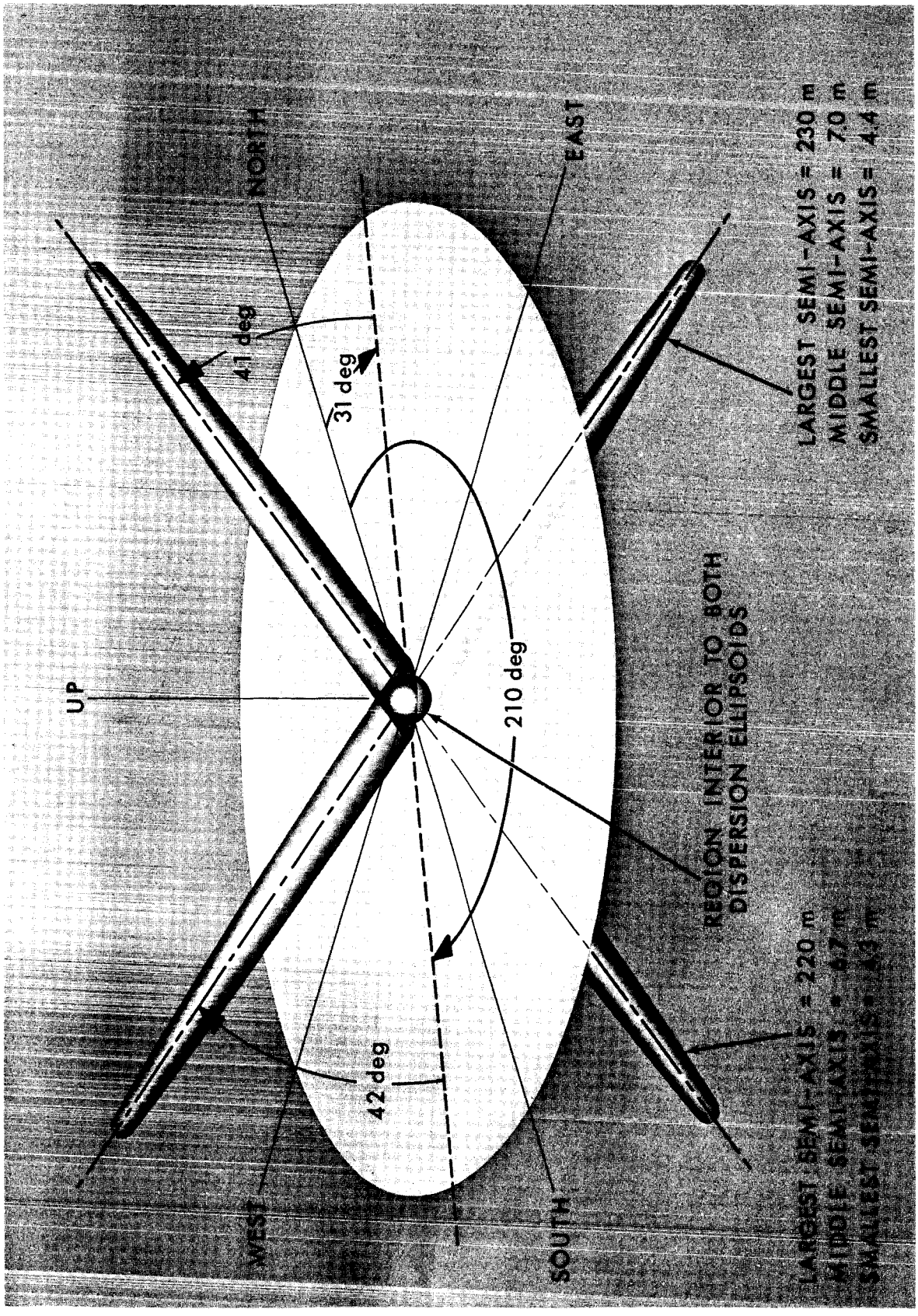

Fig. 1. Dispersion ellipsoids of station-location error for single passes eastward and westward of station (range rate, equatorial station, satellite altitude = 1860 km)

Table 10. Semi-axes of error ellipsoids for single passes

Station latitude, deg	Type of pass	Range only			Range rate only		
		LSA, m	MSA, m	SSA, m	LSA, m	MSA, m	SSA, m
Satellite altitude = 186 km (100 nm)							
0	−	479	22.3	20.2	79.9	2.80	1.57
	0	116,000	29.7	17.3	4690	1.77	1.34
	+	476	22.2	20.1	80.0	2.80	1.57
7.5	−	474	23.4	19.7	78.8	2.74	1.54
	0	47,700	29.5	17.3	3860	1.78	1.00
	+	468	22.4	19.9	77.4	2.75	1.55
15	−	472	23.0	19.0	73.3	2.64	1.50
	0	9,900	29.4	16.3	1260	1.79	1.05
	+	456	22.8	19.3	75.7	2.58	1.47
22.5	−	489	24.2	17.9	73.8	2.34	1.35
	0	5,760	29.3	16.2	748	1.80	1.06
	+	448	23.7	18.3	68.3	2.43	1.39
30	−	868	27.7	17.5	114	1.93	1.18
	0	4,500	29.2	16.8	592	1.80	1.11
	+	546	26.9	17.4	74.7	2.00	1.22
Satellite altitude = 930 km (500 nm)							
0	−	193	16.3	11.0	212	6.99	3.75
	0	4,790	13.6	9.93	1,070	3.69	2.43
	+	187	15.7	11.0	205	6.86	3.72
7.5	−	177	14.9	11.1	179	6.33	3.55
	0	5,870	13.6	9.95	1,145	3.69	2.43
	+	192	16.4	11.0	210	7.05	3.77
15	−	161	13.3	11.3	114	5.53	3.28
	0	2,050	13.6	9.93	941	3.69	2.43
	+	182	15.8	11.0	189	6.76	3.67
22.5	−	219	13.6	11.8	144	4.91	2.92
	0	1,140	13.6	9.91	669	3.68	2.41
	+	161	14.3	11.1	151	6.07	3.44
30	−	552	13.5	10.4	338	3.74	2.54
	0	884	13.6	10.3	560	3.68	2.50
	+	138	12.1	11.0	101	4.69	2.98
Satellite altitude = 1860 km (1000 nm)							
0	−	106	10.4	8.45	230	6.97	4.38
	0	1,560	9.68	7.89	596	4.94	3.49
	+	103	10.2	8.48	220	6.77	4.31
7.5	−	105	9.85	8.56	216	6.51	4.23
	0	3,790	9.68	7.93	638	4.94	3.49
	+	102	10.4	8.46	218	6.91	4.36
15	−	108	9.14	8.78	203	5.98	4.00
	0	931	9.69	7.90	652	4.93	3.49
	+	99.3	10.3	8.48	208	6.85	4.33
22.5	−	131	9.14	8.46	221	5.45	3.75
	0	691	9.69	7.88	719	4.93	3.48
	+	93.9	9.69	8.61	182	6.40	4.15
30	−	17,500	9.66	8.37	3580	4.97	3.62
	0	415	9.69	8.17	673	4.93	3.60
	+	95.2	9.12	8.91	162	5.62	3.91

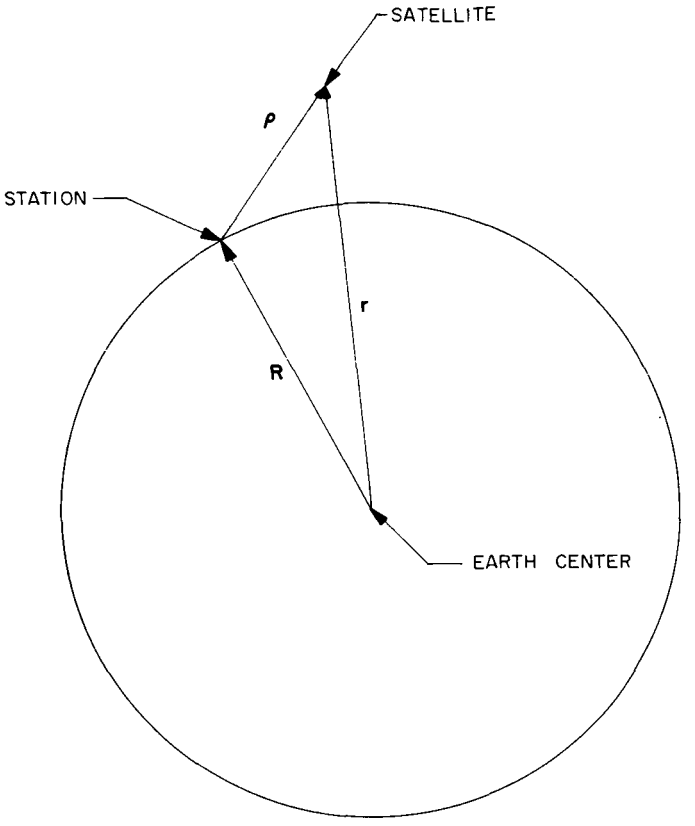

Fig. 2. Geometry for assumptions of nonoverhead pass and nonrotating Earth

direction). The direction of this vector may best be interpreted as the direction along which a tape-measure is stretched to locate the station. This vector is perpendicular to the direction of $\boldsymbol{\rho}$ and $\boldsymbol{\rho} \times \mathbf{V}$ and, using simple identities, may be written

$$\nabla D = \frac{\boldsymbol{\rho} \times (\boldsymbol{\rho} \times \mathbf{V})}{|\boldsymbol{\rho}|^3} \tag{9}$$

For the overhead case, $\boldsymbol{\rho}$ and $\mathbf{V}$ are always coplanar; therefore, no measurements are made normal to this plane, or in the $\boldsymbol{\rho} \times \mathbf{V}$ direction.

Certain properties of this measurement vector are best described in a satellite-oriented system. Let the station coordinates be described by

R = distance from center of Earth

ν_0 = true anomaly of satellite when closest to station (arbitrarily defined for circular orbits)

ψ_0 = angle at Earth center between station and satellite at closest approach.

For the geometry of this system, see Fig. 3. The satellite position is now described by only one parameter, ν, and the following equation results:

$$d\mathbf{R} = dR\mathbf{i} + Rd\nu_0\mathbf{j} + Rd\psi_0\mathbf{k} \tag{10}$$

where

$d\mathbf{R}$ = vector from center of Earth to station

$\mathbf{i}$ = unit vector outward from Earth

$\mathbf{j}$ = unit vector along satellite direction

$\mathbf{k}$ = unit vector across satellite direction

The components of ∇D are $\frac{\partial D}{\partial R}, \frac{1}{R}\frac{\partial D}{\partial \nu_0}, \frac{1}{R}\frac{\partial D}{\partial \psi_0}$, where

$$\frac{\partial D}{\partial R} = n\left\{\frac{a\cos\psi_0\sin(\nu-\nu_0)}{\rho} + \frac{Ra\cos\psi_0\sin(\nu-\nu_0)}{\rho^3} \times [R - a\cos\psi_0\cos(\nu-\nu_0)]\right\}$$

$$\frac{\partial D}{\partial \nu_0} = n\left[\frac{R^2a^2}{\rho^3}\cos^2\psi_0\sin^2(\nu-\nu_0) - \frac{Ra}{\rho}\cos\psi_0\cos(\nu-\nu_0)\right]$$

$$\frac{\partial D}{\partial \psi_0} = n\left\{-\frac{Ra}{\rho}\sin\psi_0\sin(\nu-\nu_0) \times \left[1 + \frac{Ra}{\rho^2}\cos\psi_0\cos(\nu-\nu_0)\right]\right\} \tag{11}$$

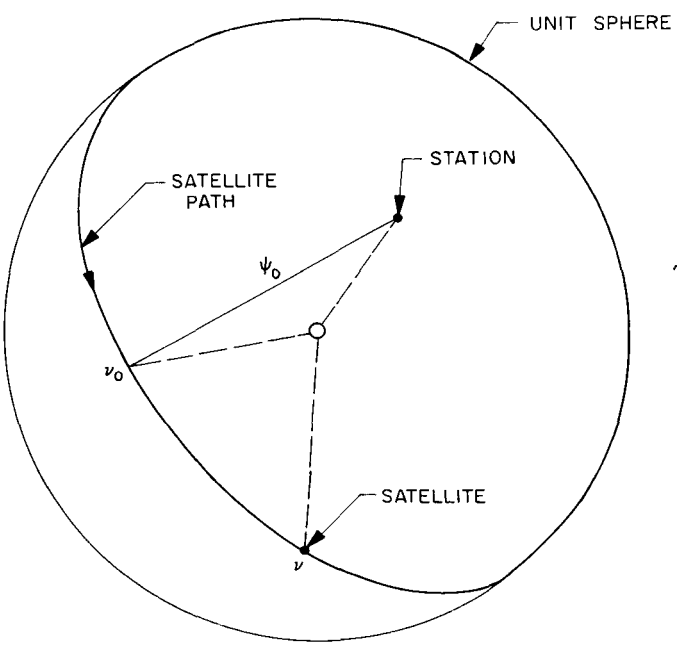

Fig. 3. Satellite–station spherical coordinates

where, since circular orbits only are under consideration,

$$a = \text{orbit semi-axis} = |\mathbf{r}|$$

$$R = |\mathbf{R}|$$

$$\rho = |\boldsymbol{\rho}|$$

$$n = \text{satellite mean motion} = \frac{V}{R}$$

From the discussion above, note that, for a given station and orbit, if ∇D at a given value $(\nu - \nu_0)$ is represented by (a, b, c), then ∇D at $-(\nu - \nu_0)$ is $(-a, b, -c)$. When observations are symmetrical about ν_0, this symmetry results in a normal equation coefficient matrix of the form

$$\begin{bmatrix} j_1^1 & 0 & j_3^1 \\ 0 & j_2^2 & 0 \\ j_1^3 & 0 & j_3^3 \end{bmatrix} \tag{12}$$

The inverse of this matrix, the covariance matrix, is

$$\text{covar}\,\mathbf{R} = \begin{bmatrix} \dfrac{j_3^3}{j_1^1 j_3^3 - j_2^1 j_2^1} & 0 & \dfrac{j_2^1}{j_1^1 j_3^3 - j_2^1 j_2^1} \\ 0 & \dfrac{1}{j_2^2} & 0 \\ \dfrac{j_2^1}{j_1^1 j_3^3 - j_2^1 j_2^1} & 0 & \dfrac{j_1^1}{j_1^1 j_3^3 - j_2^1 j_2^1} \end{bmatrix} \tag{13}$$

Note that the second coordinate of $\mathbf{R}$ is uncorrelated with the first and third. Therefore, one eigenvalue of the matrix is $1/j_2^2$, and its eigenvector is (0, 1, 0); i.e., it lies along the flight-path direction at satellite closest approach.

The remaining eigenvectors are in a plane normal to the flight-path direction at closest approach. The measurement-direction component in this plane varies throughout a pass and may be described by its elevation angle from the horizontal plane and by the relative sensitivity of each measurement. A typical case is illustrated in Fig. 4. The slope S (tangent of the elevation angle) of those measurements in this plane lies between the limits

$$S_s \geq S \geq S_{ca}$$

and

$$S_{ca} \geq \tan E_{max} \tag{14}$$

where

E_{max} = maximum elevation angle of satellite

S_{ca} = slope of ∇D projection, satellite at closest approach

S_s = slope of ∇D projection, satellite at any point between overhead and set positions

S = slope of ∇D projection, satellite at set position

The following expressions result:

$$S_s = \left[1 - \left(\frac{R}{a}\right)^2\right] \frac{1}{\tan \psi_0}$$

$$S_{ca} = \frac{1 - \left(\dfrac{R}{a}\right) \cos \psi_0}{\left[1 - \left(\dfrac{R}{a}\right) \cos \psi_0 + \left(\dfrac{R}{a}\right)^2\right]} \frac{1}{\tan \psi_0}$$

$$\tan E_{max} = \left[1 - \left(\frac{R}{a}\right) \frac{1}{\cos \psi}\right] \frac{1}{\tan \psi_0} \tag{15}$$

Similar statements hold true for the pass from rise to closest approach, since the vectors are merely the negatives of those after closest approach. The result of combining these measurements in this plane is that one eigenvector is always between the limits shown.

In summary, the semi-axes of the doppler single-pass error ellipsoid are determined by the following rules:

1. The *smallest* semi-axis lies in the horizontal plane in the direction of the satellite velocity at closest approach.
2. The *middle* semi-axis is determined as the resultant of a two-dimensional series of nearly parallel measurements in a vertical plane containing the closest-approach point. The narrow spread of the elevation angle of these measurements is given by specified inequalities.
3. The *largest* semi-axis is determined to approximately the magnitude of the MSA over the sine of the spread of the measurement vectors (projected on the same vertical plane).

Examination of the rotating-Earth case reveals no significant departure from these results, except in the obvious case of an overhead pass.

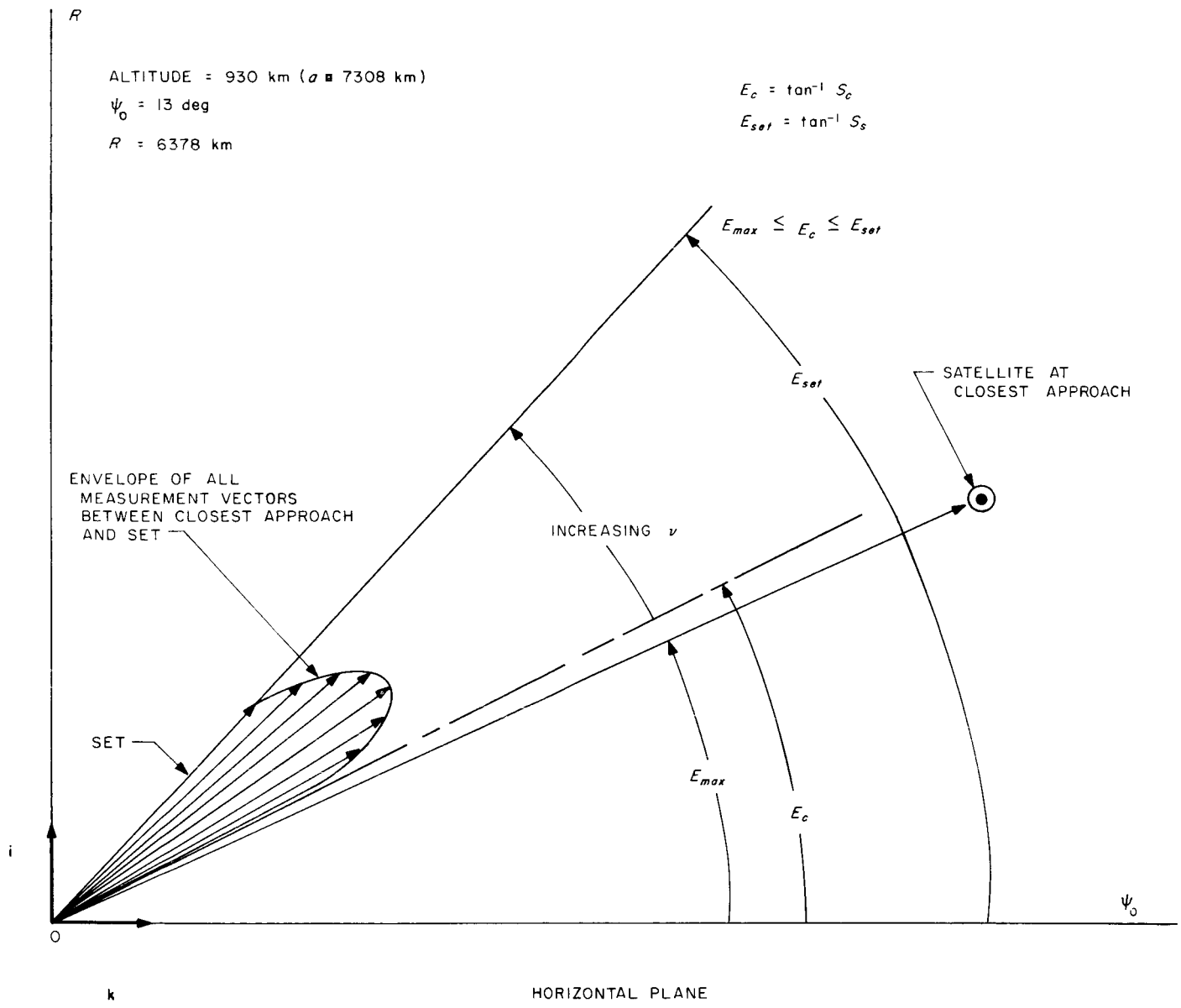

Fig. 4. Relation of measurements determining R and ψ_0

V. CRITICAL ACCURACY VARIATION FOR SINGLE PASSES

A. Summary of Single-Pass Results

It was shown in Section IV that the middle semi-axis of the three-dimensional error ellipsoid $\delta \mathbf{x}^T \Gamma_x^{-1} \delta \mathbf{x} = 1$ is the most useful single parameter characterizing the accuracy obtainable in a particular *single* pass when data are obtainable on one or more other passes. The values of all three semi-axes of the 1-σ error ellipsoid for the single passes examined are summarized in Table 10. Many interesting observations may be made by careful study of these results.

B. Variation of Middle and Largest Semi-axes with Type of Pass, Latitude, and Altitude

1. Variation of Middle Semi-axis with Type of Pass

It is noteworthy that, for the *range only* cases, there is no significant variation of the MSA with the geometry of the pass. The corresponding variation for the *range rate only* cases is also fairly minor, although here we find that the MSA values are almost always largest for the case where the satellite is west of the station (+), and always smallest for the overhead case.

2. Variation of Largest Semi-axis with Latitude and Type of Pass

The largest semi-axis is a strong function of the geometry of the pass. The *satellite east* and *satellite west* figures are substantially the same. The overhead-pass LSA values are always large and become systematically larger as the orbit altitude is decreased, because of the shorter duration of the passes. The moderate irregularity in the variation with station latitude is not considered to be of importance. The significant increase of LSA as the station latitude approaches 0 deg is not surprising, since the effect of the Earth's rotation during the pass is small because of the symmetry.

3. Variation of Middle Semi-axis with Latitude

Examination of Table 10 reveals that the *range only* MSA values have no important variation with latitude, and that insignificant variation occurs for the overhead passes. The *range rate only* MSA's are similarly insensitive for overhead passes, but are somewhat more latitude-dependent than the *range only* cases for the nonoverhead passes.

4. Variation of Middle Semi-axis with Altitude

There is a significant variation of the middle semi-axis with satellite altitude, as shown in Fig. 5. It is interesting to note that the MSA at a 1860-km altitude is 3 times larger than the same semi-axis at 186 km for the case of *range rate*, whereas at 1860 km the MSA is 3 times smaller than at 186 km for *range only*. The duration of the view periods for each altitude is given in Table 11. It will be noted that either range or range-rate measurements give excellent accuracy for relatively high orbital altitudes. Angular observations, if taken, would degrade in effectiveness with increasing altitude.

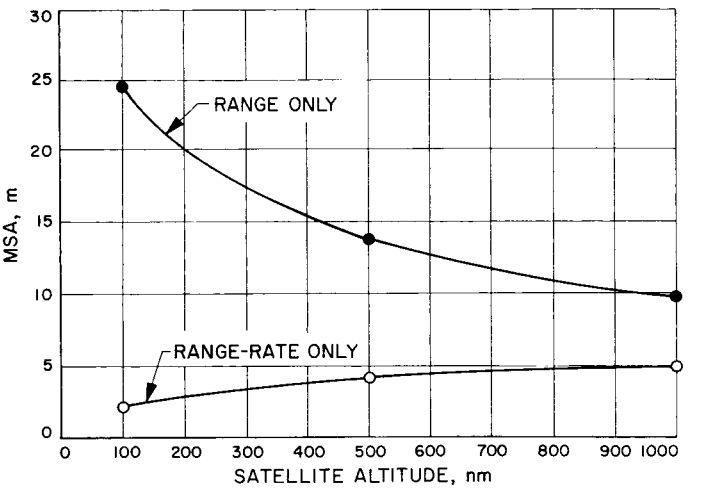

Fig. 5. Variation of middle semi-axis with altitude for overhead pass at equatorial station

Table 11. Length of view periods for overhead pass at equatorial station

Altitude, km	Length of pass, sec
186	402
930	955
1860	1649

C. Comparison of Range and Range-Rate Measurements

In a system where both range and range-rate measurements are available, it appears that the biases of the ranging system could be calibrated by means of the

doppler measurements. In the situation discussed here, range biases are assumed to be negligible. Figure 6 is a graph of the standard deviation required of range data in order that the MSA from a single overhead pass at an equatorial station will be equal to the corresponding situation for range rate only. For the region above the curve, the most information comes from range rate.

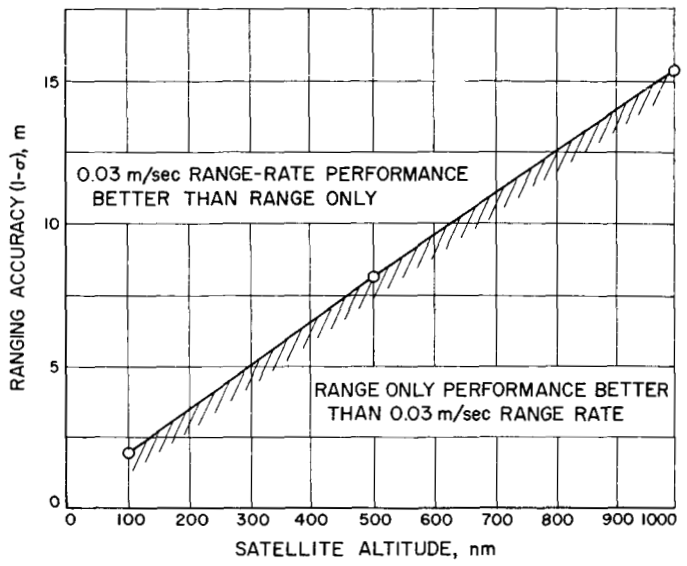

Fig. 6. Ranging accuracy required to obtain middle semi-axis equal to that obtainable with range rate of 0.03 m/sec (1-min sampling rate)

Figure 6 presents a case which is somewhat too optimistic as to the value of the range measurements, since it will probably be necessary to solve for a small random bias on each pass of range data. Even so, a *range rate only* system appears to be competitive with a *range only* system.

Figure 7 indicates the range and range-rate accuracies necessary to achieve an MSA of 5 m as a function of satellite altitude for the overhead pass at an equatorial station.

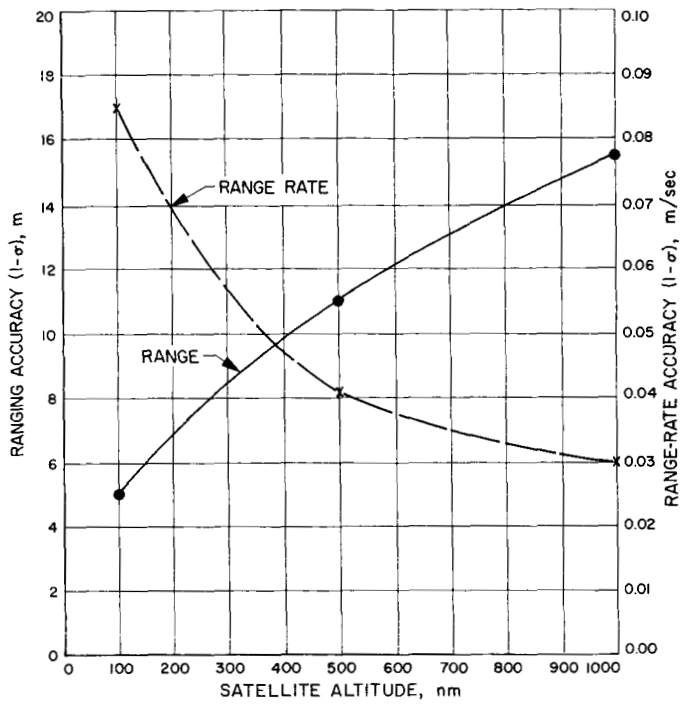

Fig. 7. Data standard deviations required to obtain middle semi-axis of 5 m (accuracies normalized to 1-min sampling rate)

VI. CONCLUSIONS

In this Section, we attempt to summarize the significance of this Report and the degree to which its results and insights depend upon the rather restrictive assumptions on which the computations are based. Next, this restricted problem is contrasted with the larger problem of implementing a calibration-satellite system. Finally, some observations are made on the problem of the overall best estimate of the trajectory (BET).

A. Primary Results

The method used to interpret the value of a single pass of tracking data in locating the station, and also the visualization of favorable geometry, are substantially independent of the simplifying assumptions. The actual values of the smaller semi-axes of the 1-σ error ellipsoids are certainly subject to some increase in the complete solution, which includes the satellite-orbit determination, the station systematic errors, and the perturbing forces. We expect that the results presented here will show the proper relationships between the important parameters and data types.

B. Restrictive Assumptions

The assumption of adequate time synchronization of stations in the feasible era of such satellites appears to be sound. Timing errors of 1 msec could contribute errors as large as 8 m in station location; however, if useful, an improvement in time synchronization of one or two orders of magnitude is attainable. The unstated assumptions of the fixed location of the Earth's spin axis with respect to the crust, and of the very slow relative motion of points on the Earth's crust, are not likely to create short-term problems when 5 m is the accuracy goal.

With respect to the measuring of a station's coordinates to 5 m, the most dubious assumption is that of a perfectly known orbit. Here, further study is required to determine the best selection of orbit parameters and of spacecraft shape, attitude control, and reflecting properties, in order to optimize the accuracy capabilities. We expect that a relatively high altitude (over 400 nm) will prove most favorable, since the magnitude of effects due to atmospheric drag and the harmonics of the Earth's potential field is lower. At the same time, the single-pass accuracies degrade only mildly with increasing altitude. An additional advantage in the use of higher altitudes is the capability of viewing the satellite on two or three consecutive passes.

C. The Total Problem

Here, the most appropriate comment is that implementation of the spacecraft design and the ground systems for taking and processing the data obtained and disseminating the results is a formidable but feasible task. Centralization of data processing for orbit computations seems essential. In the steady state, it is probable that locally accurate descriptions of an established orbit could be compactly communicated to other locations for rapid analysis of the results of a series of passes.

The spacecraft design is almost completely beyond the scope of this Report, except for the few remarks on orbit-parameter selection. The dissemination of results and the adoption of standards and reference systems present no new problems, but would be a source of much discussion.

NOMENCLATURE

A	transformation matrix
a	orbit semi-axis $= \lvert \mathbf{r} \rvert$
B	transformation matrix
BET	best estimate of trajectory
D	doppler measurement
∇D	gradient of doppler measurement
E	exponent of 10 (e.g., $0.178\ \mathrm{E}\ -3 = 0.178 \times 10^{-3}$)
E_c	elevation angle of projection of ∇D at closest approach
E_{max}	maximum elevation angle of satellite
E_{set}	elevation angle of projection of ∇D at set position
h	altitude
$\mathbf{i}$	unit vector outward from Earth
J	basic normal matrices for one orbital pass
$\mathbf{j}$	unit vector along satellite direction
j	elements of matrix J
$\mathbf{k}$	unit vector across satellite direction
LSA	largest semi-axis
MSA	middle semi-axis
n	satellite mean motion $= V/R$
$\mathbf{R}$	vector from center of Earth to station
R	distance from center of Earth, km $(= \lvert \mathbf{R} \rvert)$
$\mathbf{r}$	vector from center of Earth to satellite
$(r, \phi, \lambda)^T$	station coordinates $\boldsymbol{\varphi}$ in radius-latitude-longitude system
S	slope of ∇D projection, satellite at any point between overhead and set positions
S_{ca}	slope of ∇D projection, satellite at closest approach
S_s	slope of ∇D projection, satellite at set position
SSA	smallest semi-axis
T	(superior) transpose of matrix
$\mathbf{V}$	satellite velocity vector
W	inverse of data-noise covariance matrix
$(x_1, x_2, x_3)^T$	local east and north horizontal directions and local vertical directions
$\mathbf{y}$	observation vector
Γ_x	ellipsoid of concentration
δ	deviation from reference station coordinates or observable quantities
ν_0	true anomaly of satellite when closest to station (arbitrarily defined for circular orbits)
$\boldsymbol{\rho}$	station-to-satellite vector
ρ	$\lvert \boldsymbol{\rho} \rvert$
$\boldsymbol{\varphi}$	coordinates of tracking station
ψ_0	angle at Earth center between station and satellite at closest approach
$\triangleq$	equal by definition

REFERENCES

1. Mancini, A., and Brown, D. C., "Calibration Satellite," paper presented at *Fourth Joint AFMTC–Range User Data Conference*, February 26–28, 1963, Air Force Conference Facility, Orlando Air Force Base, Florida.

2. Reich, A., and Schucker, S., "Radar Applications to Geodesy," paper presented at *IRE Ninth Annual East Coast Conference on Aerospace and Navigational Electronics*, Institute of Radio Engineers, Inc., October 22–24, 1962, Baltimore, Maryland.

3. Hamilton, T. W., "Applications of Celestial Mechanics to Spacecraft Flight," pp. 25–27, NASA SP-15, *Proceedings of the NASA–University Conference on Science and Technology of Space Exploration*, November 1–3, 1962, Chicago, Illinois.